ORIGINAL ARTICLE

Journal Section

Evaluation and consideration of local specimen material properties in lifetime prediction of short fibre reinforced PA6T/6I

Gabriel Stadler[1] | **Andreas Primetzhofer**[3*] | **Gerald Pinter**[2] | **Florian Grün**[1]

[1]Chair of Mechanical Engineering, Montanuniversität Leoben, Leoben, Styria, 8700 , Austria

[2]Chair of Polymer Testing, Montanuniversität Leoben, Styria, 8700, Austria

[3]Polymer Competence Center Leoben, Leoben (PCCL), Styria, 8700, Austria

Correspondence
Andreas Primetzhofer, Polymer Competence Center Leoben (PCCL), Leoben, Styria, 8700, Austria
Email: andreas.primetzhofer@pccl.com

Funding information
This research was funded by Austrian Research Promotion Agency (FFG) grant number 854178. The PCCL is founded by the Austrian Government and the State Governments of Styria, Lower and Upper Austria.

To exploit the full material potential of short fibre reinforced PA6T/6I, specific component calculations including anisotropic material behaviour is necessary. For this, different failure criteria and fatigue models are used to describe the behaviour during a component service life. This paper deals with the determination and consideration of fibre orientations for failure criteria and fatigue calculations. Therefore, a novel method to determine fibre orientation (FO) distributions across injection moulded plates, is proposed. The developed method allows a forecast of FOs for different specimen extraction positions and angles on injection moulded plates by using only a few measured reference points. As a result, fatigue models can be calibrated with the strength values and the corresponding FO, calculated for fracture position. The performed tests show a non-negligible influence of failure positions, due to fibre orientation distributions along the specimens. So, the FO determination method delivers an improvement in strength values estimation.

[*]Equally contributing authors.

KEYWORDS
short fibre reinforced polyamide, fibre orientation, failure, local material behaviour, microstructure, testing

1 | INTRODUCTION

Lightweight applications require a specific type of materials to get a high system performance. Especially in the automotive sector, several metallic and non-metallic materials, including short fibre reinforced polymers (sfrp), are used. Previous investigations about the fatigue behaviour of sfrp for such purposes have been performed and published. A number of studies have shown, that the factors fibre orientation [1,2,3,4,5,6], notches [5,7,8], temperature [9,10,11,12], moisture [13,14] and multiaxial loadings [15,16,17] have main impact on the fatigue strength. To estimate a bearable number of load cycles, several simulations (e.g. injection moulding and structure simulations) have to be performed [18]. Based on the results of an injection moulding simulation, the fibre orientation is defined for structural analysis. The material parameters for these service time estimations are determined with tensile and fatigue tests. To define a material load capacity, local stresses at different load cases as well as material strengths have to be determined. The bearable load capacity of anisotropic, reinforced materials strongly depends on the local fibre orientation. Consequently, knowledge about the local material structure and its mathematical description is important for consideration in simulations. Azzi et. al proposed in [19] a model for local strength calculations using the loading angle, known as the *Tsai-Hill-criterion*. Equation 1 describes the *Tsai-Hill-criterion* model mathematically.

$$\sigma_\phi = [\frac{cos^2(\phi)(cos^2(\phi) - sin^2(\phi))}{\sigma_1^2} + \frac{sin^4(\phi)}{\sigma_2^2} + \frac{cos^2(\phi)sin^2(\phi)}{\tau_{12}^2}]^{-1/2} \tag{1}$$

σ_1, σ_2 and τ_{12} are the longitudinal, transversal and the shear strengths of the investigated material. The loading angle ϕ varies from 0° to 90° and corresponds to the specimen's extraction angle on the plate. σ_ϕ represents the strength of the material for an investigated loading angle (ϕ).
To consider the fibre orientation in lifetime calculations, independent of the specimen's position on the plate for a certain loading angle, a method has been developed by Gaier et al. [20] (equation 2, figure 1).

$$w_i = w_0 \cdot exp(m \cdot \lambda_i) \tag{2}$$

This model excepts an exponential connection between the fibre orientation and material properties and is empirically determined. The parameter m represents the slope of the curve, the parameters λ_i are the fibre orientations, in the main loading direction. A calculated material parameter w_0 (Young's modulus, tensile and fatigue strength, etc.) with (theoretically) fully transversal aligned fibres, serves as a reference point. Gaier et al. proposed in [21] a model including the critical cutting plane angle (δ) and material parameters for two fibre orientations (w_1, w_2) (equation 3). The material values (w_1, w_2) for this model are calculated by using equation 2 with the fibre orientations λ_1 and λ_2. The cutting plane is virtually rotated around every node of a finite element simulation model. During these rotations, the local stresses and material strengths on this plane are compared for each angle. If the gap between the local stresses and bearable strength (both normal to the cutting plane) becomes a maximum, the *critical cutting plane* (angle δ) is reached. The result is a material parameter, for this, critical angle (w_{mat}) determined with equation 3.

$$w_{mat} = \frac{w_1 + w_2}{2} + \frac{w_1 - w_2}{2} cos(2\delta) \tag{3}$$

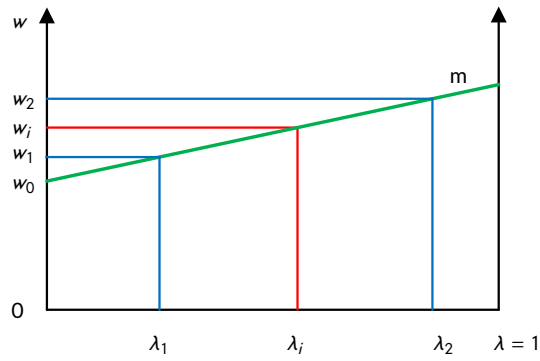

FIGURE 1 Influence of fibre orientation on material parameters according to [20]

As a result of these two methods, the position of the critical cutting plane is calculated by the local stresses and anisotropic strengths based on the local fibre orientation tensor.
Component fatigue calculations are actually done with these methods, delivering reliable results [18,22]. The required material data for tensile and fatigue behaviour is determined on specimens with a non-homogeneous, quasi layered fibre structure. Such a structure is a known phenomenon in thin injection moulded plates made of sort fibre reinforced polymers [3,23,24]. A growing body of literature has investigated the influence of fibre orientations on material strengths, but only a few studied the fibre distribution in the specimen for fatigue [25,26]. Further, only the extraction angles are considered for the failure criteria, independent of the local fibre orientation distribution across the plate. As a result, different local fibre orientations on the fracture positions come along with changing extraction angles. Consequently, the validity of standard criteria (e.g. *Tasi-Hill-criterion*) gets lost with different extraction positions on injection moulded plates. Consequently, a calculation method for the fibre orientation at specific positions and extraction angles has been developed. In this paper, on the one hand, the fibre orientation distribution and on the other hand, failure areas are investigated. The purpose of these determinations is to show the influence of the local fibre orientations, depending on the specimen's extraction positions on injection moulded plates and the effect on material model parameters. Moreover, a calculation of the associated fibre orientation for a measured strength can be done by using the developed calculation method. So, this novel approach improves the prediction of the fatigue strength for certain fibre orientations up to 35%.

2 | EXPERIMENTAL

The investigated material for these studies is a partial aromatic polyamide PA6T/6I with a glass fibre content of 50% by weight. The material has an average fibre length of 200 μm. To evaluate the material behaviour of the sfrp for different fibre orientations, fatigue and tensile tests have been performed. For this, bone shaped specimens, shown in figure 2, were milled from a 100x100x2 mm injection moulded plate at different positions and angles [27]. Figure 3 shows the extraction angles and positions of the specimens on the plate. The 2 mm thick plate offers a high fibre orientation for the specimens. The extraction positions of the specimens have been chosen to capture a fibre orientation distribution along the plate. Since a nearly homogeneous fibre orientation along x-direction (flow-direction) compared to the distribution along the y-direction has been measured (figure 8), a larger distance between the *longitudinal* spec-

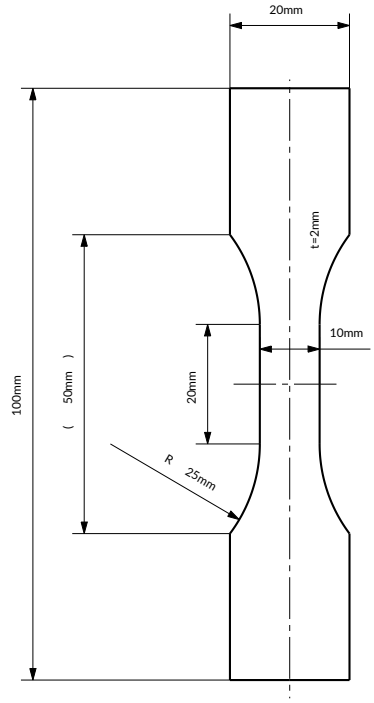

FIGURE 2 Specimen shape for tensile and fatigue tests

imens (compared to *transversal* specimens) has been chosen. So, there is a higher fibre orientation in the longitudinal specimens. In this publication, the *longitudinal* specimens (figure 3-1) are declared with, *left (L)*, *middle (M)* and *right (R)* along the y-direction. The transversal specimens are named *lower (L)*, *middle (M)* and *upper (U)* (figure 3-2 and 3). The angle of 45° has been chosen to get a fibre orientation angle between 0° and 90° without cutting edges of the specimens (which would be the case with 30° or 60° specimens, figure 3-4). By simply rotating the specimen around the plate centre (which is a standard method), only the fibre orientation along the extracted specimen can be captured for different angles. Since the averaged fibre orientation in the centre of the plate is about 0.4 (x-direction) and 0.56 (y-direction), there is a low range between longitudinal and transversal fibre orientation for model calibrations. To capture a wide range of fibre orientations in the specimens the positions, shown in figure 3, have been chosen for longitudinal and transversal. Consequently, the fibre orientation model calibration needed to be adapted for a higher reliability.

To determine the fibre orientation for the whole plate area, μCT scans have been performed at specific positions, which are shown in figure 4. The scanning points are located concentrically to point P3 along with two circles, whereby point P5-1 uses the overflow cavity for a complete sample. This sample arrangement captures the fibre orientation development along the flow direction as well as the development perpendicular to the flow direction (plate width). Since the specimens for the tensile and fatigue tests have been taken from different positions across the plate, shown in figure 3, also the fibre orientation needed to be investigated at these positions. Consequently, position P-1 represents the orientation of the 0° (longitudinal, *left-right*) specimens, P-2 the 90° (transversal) specimens and P-3 the 45° specimens. The size of the μCT-specimens is 4x4x2 mm, for representative fibre orientation measurement results

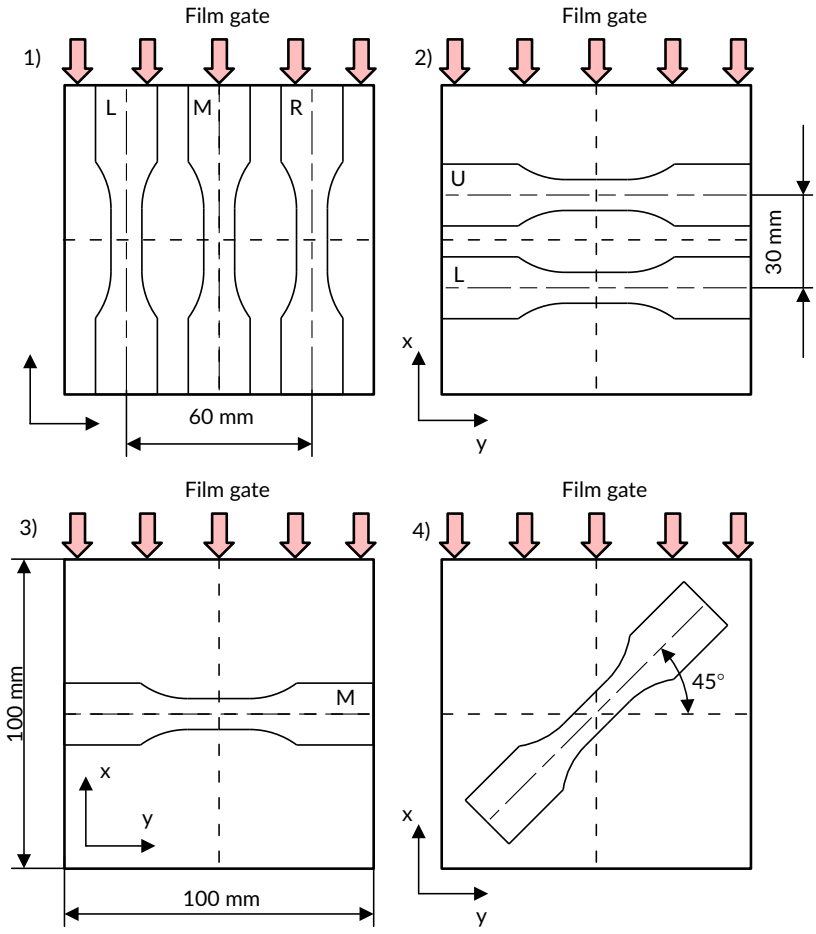

FIGURE 3 Specimen extraction positions on the plate: 1) *longitudinal specimen- left*, *middle*, *right*, 2) *transversal specimen-upper*, *lower*, 3) *transversal specimen-middle* 4) 45° *specimen*

at the relevant regions. A GE Phoenix Nanotom 180 computer tomograph has detected the fibres with Molybdenum target using a current of 115 μA and an acceleration voltage of 80 kV. The volume size of the detected areas is 2μm/voxel. Volume graphics and an open-source software from FH-Wels[28] prepared the data.

For the mechanical tests, two different types of test rigs have been used. Tensile and fatigue tests were performed on an electromechanical testing machine, BOSE® Electroforce AT3550. Figure 5 shows the test rig with a clamped specimen. Additionally, a hydraulic test rig, based on a module frame with an Instron® control unit, performed fatigue tests (figure 6). An extensometer from Instron® with a measure length of 12.5 mm has captured the local strains (for tensile tests) and is implemented in both test rigs. Tensile tests were performed with a displacement rate of 2 mm/min according to DIN ISO 527-1 leading to a strain rate of $6.6 \cdot 10^{-4} s^{-1}$. The environmental conditions for all these tests (also fatigue tests) are defined with a relative humidity of 50 % and a temperature of 23 °C. For every loading angle, three tensile tests have been performed. The results have been averaged for the determination of the material parameters (figure 13). Fatigue tests with a frequency of 10 Hz at a stress ratio of R=0.1 were performed. The specimens

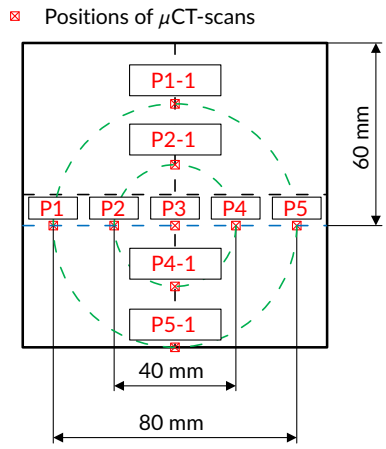

FIGURE 4 Positions of μCT-scan samples on the plate

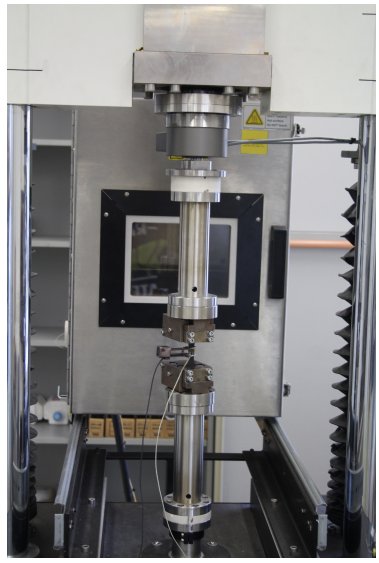

FIGURE 5 Electrodynamic test rig with clamped specimen

have been tested, until fracture occurs. The fracture positions usually are located at the end of the parallel area of the specimens, also for tensile tests. Figure 7 shows the fracture areas of specimens after testing. These positions, provoked by the local fibre orientation combined with a stress concentration, are considered in the material model calibration. So, the material model must be calibrated for the fibre orientation in these areas. For every test series, a minimum number of seven tests have been performed at different load levels. To get the fatigue parameters, averaged values of the test points are considered.

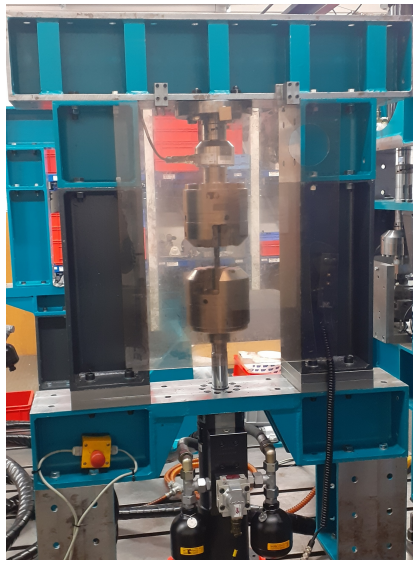

FIGURE 6 Hydraulic test rig with clamped specimen

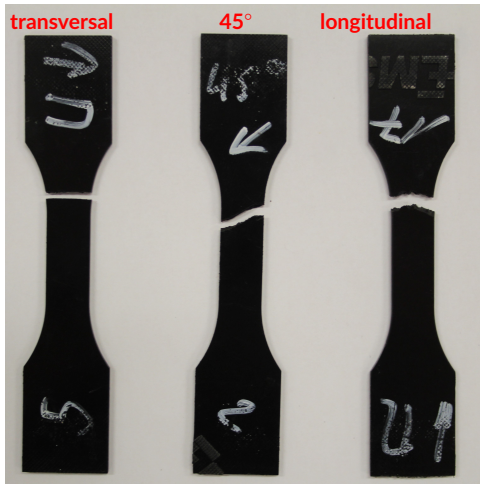

FIGURE 7 Fracture areas of the specimens (examples of specimens after cyclic testing)

3 | RESULTS

3.1 | Fibre orientation analysis

The results show an inhomogeneous distribution through the plate thickness at the investigated points due to different local flow conditions in the injection moulding process, plotted in figure 8 and figure 9. With the exception of a thin skin layer, there are high oriented areas on the top and bottom of the plate. Figure 8 shows, that the main orientation

decreases to the middle layer along the plate centre path. However, there is symmetry around the centre of the plate. As a result, the fibre orientation varies along the cross area of the specimens. To get a fibre orientation tensor for every specimen, the mean values are considered. Since the values, which are not in the main diagonal of the matrix, are negligible (compared to the main diagonal entries), they are not considered for further investigations. The fibre

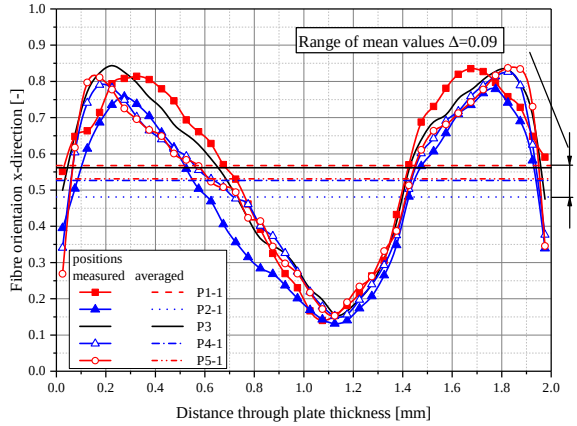

FIGURE 8 Fibre orientation along flow direction (P1-1 to P5-1)

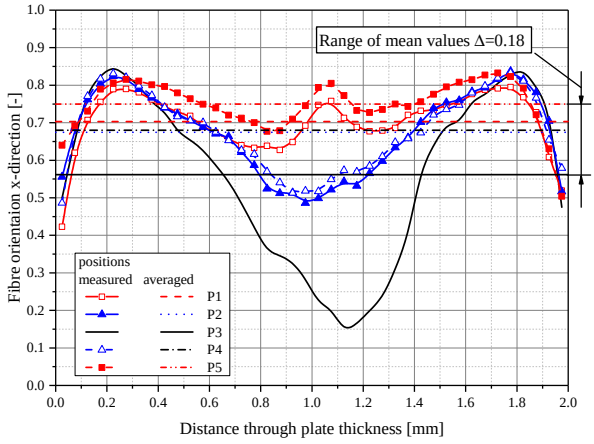

FIGURE 9 Fibre orientation perpendicular to flow direction (P1 to P5)

orientation along the flow direction (P1-1 to P5-1) shows a nearly constant distribution of the mean FO values (figure 8 and figure 11). But the fibre orientation distributions and mean values across the plate width (P1 to P5) is varying significantly (figure 9). Accordingly, there is a main effect on the local fibre orientation depending on the extraction position for longitudinal specimens (figure 9). Since these averaged fibre orientations are considered for lifetime calculations, there should be paid more attention to them. The difference of mean x-direction fibre orientation values between the *middle* and the *left-right* specimens is about 25 % (figure 4: P3 and P5). The averaged fibre orientations at the positions along the flow path (P1-1 to P5-1) and the plate width (P1 to P3) provides information about the

distribution across the plate (figure 11). The fibre orientation is also increasing outward the centre across the plate width due to a shear flow distribution (figure 10).

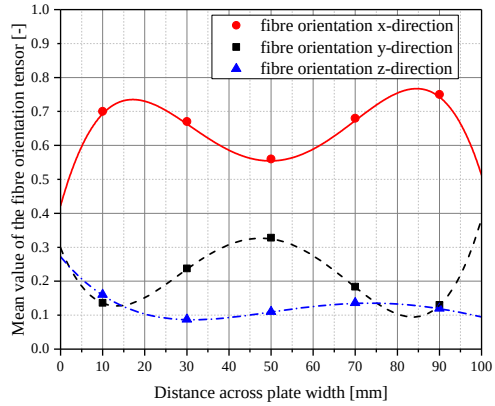

FIGURE 10 Fibre orientation along plate width (corresponds to y-direction)

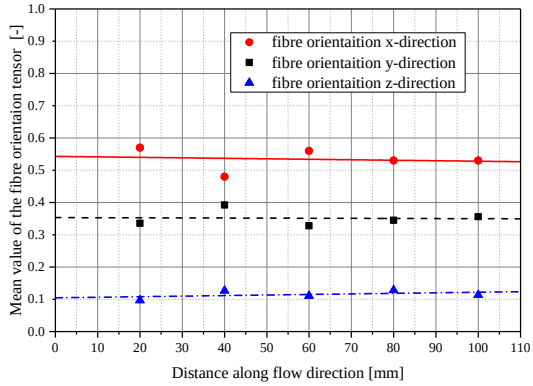

FIGURE 11 Fibre orientation along plate length (flow path corresponds to x-direction)

3.2 | Mechanical tests

Figure 12 and figure 13 show the influence of the specimen position and the angle on the tensile and fatigue test results. The results in the graphics are normalized to the fatigue strength of longitudinal (*left-right*) specimens. The tests confirm significant differences between the orientation angle and the fatigue strength[3]. It can be shown, that the gap between the stress amplitudes at 10^6 cycles increases exponentially (figure 12 and figure 17). Since the *Gaier-model* assumes an exponential connection between the fibre orientation and strength properties, the fibre orientations of the specimens at the fracture points are investigated. The S/N-curves are calculated for a survival probability of 50%. The dispersion for the investigated positions are shown in table 3.2.

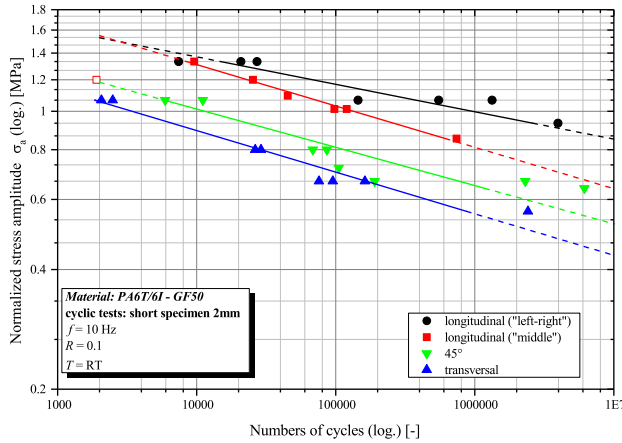

FIGURE 12 S/N-curves of fatigue tests

$1/T_N$	position
19.6	45°
1.6	middle
6.7	left/right
4.5	transversal

TABLE 1 Dispersions of the cyclic test results

The calculation of the dispersion T_N is done by equation 3.2 and defined by the relationship between the numbers of cycles for a survival probability of 90% (N_{90}) and 10% (N_{10})[29].

$$T_N = N_{90}/N_{10} \tag{4}$$

The tensile test results (figure 13) show differences in material stiffness between the positions except 45° and the transversal position. Since the strain measurement is done in the specimen centre, the fibre orientation in x-direction of the 45° specimen in this area is relevant for the material stiffness (figure 17). On the other hand, there are tensile strength differences of about 16% between the 45° and the transversal specimens. This gap is a result of the local fibre orientations in the fracture areas. So, there is also an exponential increase of the gap between the tensile strengths outgoing the transversal specimen. Further, it can be shown, that the S/N-curves are hardly parallel and confirm the results of[30]. By investigating the fracture positions (figure 3), marked with *x* in figure 14, one can see that there is no accordance between the positions of the μCT scan points (figure 4 and figure 14). Based on μCT scans, the local fibre orientation at the relevant fracture points needed to be calculated.

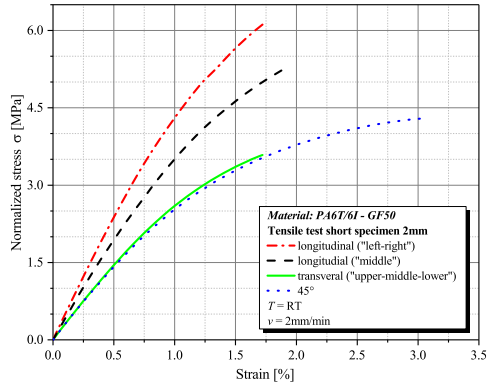

FIGURE 13 Curves of tensile tests (mean values)

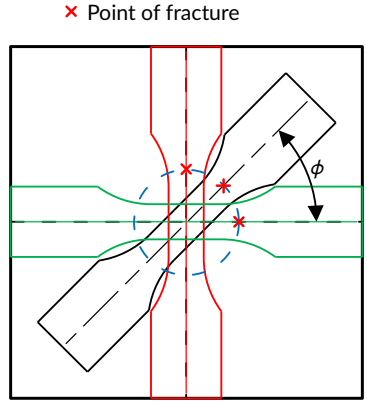

FIGURE 14 Fracture areas of the investigated extraction positions

4 | DISCUSSION

Former publications [3,31] use the *Tsai-Hill-criterion* for the lifetime prediction based on the extraction angle of the specimens on the plate. To determine the failure behaviour between the investigated angles, the failure criteria *Tsai-Hill-criterion*, according to equation 1, and *Gaier-criterion*, according to equation 3, are used. Figure 15 shows the course of the models depending on the loading angle. For the evaluation of the data using these models, strength values from *middle* as well as *left-right* for longitudinal specimens (figure 3) are considered. The results show a difference of 18.9 % for the bearable fatigue strength and 14.6 % for the fatigue static strength depending on the extraction position for an extraction angle of 0°. (figure 15). The reason for this is the inhomogeneous fibre orientation distribution along the plate width, shown in figure 10. Since the fracture positions are not located in the specimen's centre, a simple rotation delivers different fibre orientations for these positions. Figure 14 shows the positions of the fracture points, depending on the extraction angle. This effect cannot be considered in the calibration by using the proposed fatigue

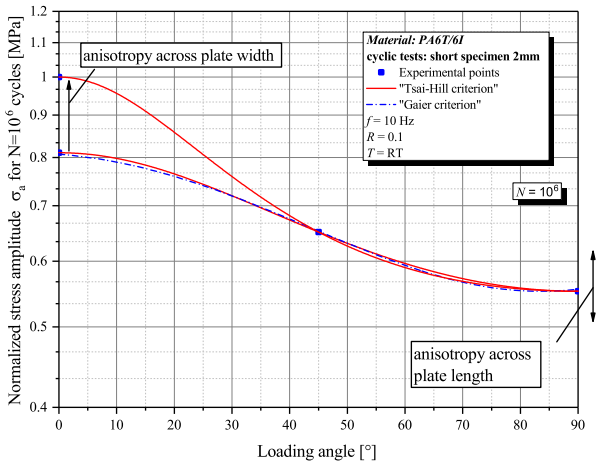

FIGURE 15 Failure criterion calibration for cyclic data

models. As a result, there is an over- e.g. underestimation of the bearable strengths at loading angles between 0 and 90°. Moreover the fibres are not fully aligned in the specimens. So, theoretically a higher strength would be possible for longitudinal loads. Consequently, higher oriented areas (e.g. in components) can't be captured with these models, calibrated with the measured data. Therefore, the fibre orientations of the fracture positions have to be considered for the failure criteria supported by μCT-scans. Using the model, proposed in this publication, the model parameter determination is improved.

The mean values of the fibre orientation for every direction are considered to get the fibre orientation development along the flow path (x-direction) and the plate width (y-direction). A polynomial function of degree 4 using equation 8 and equation 9 describes the mean fibre orientation distribution across the plate width including the changes to the plate edges. The combination of the distribution function and the coordinates of the fracture positions, determined with a circle function, the local fibre orientation for every extraction angle can be calculated. The workflow is shown in figure 16. The position of the coordinate system x'-y' is defined with Cartesian coordinates, calculated by using equation 5 and equation 6. To do this, a radius (r) is defined for a group of positions. Figure 16 shows the resulting circles from the positions of the μCT specimens. In this case, two circles can be defined. Additionally, the loading angle (ϕ) (loading direction) has to be defined.

$$x = r \cdot sin(\phi) \tag{5}$$

$$y = r \cdot cos(\phi) \tag{6}$$

Finally, the fibre orientation tensor $T(x, y)$ entries (using equation 7) which depends on the x and y-distance, are

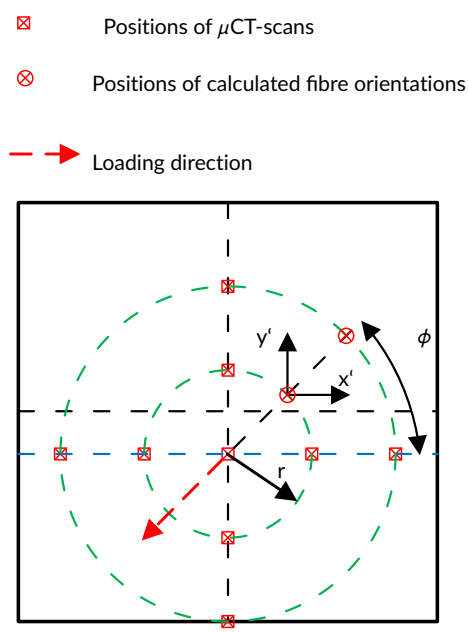

FIGURE 16 Workflow for the position calculation

calculated

$$T(x,y) = \begin{pmatrix} f_{ii}(x,y) & 0 & 0 \\ 0 & f_{jj}(x,y) & 0 \\ 0 & 0 & f_{kk}(x,y) \end{pmatrix} \tag{7}$$

by using equation 8 and equation 9. Since the fibre orientation is constant along the x-direction (shown in figure 11) the terms $P(x)$ and $O(x)$ are constants in this case.

$$f_{ii}(x,y) = ay^4 + by^3 + cy^2 + dy + P(x) \tag{8}$$

$$f_{jj}(x,y) = ky^4 + ly^3 + my^2 + ny + O(x) \tag{9}$$

The sum of the principal diagonal values equals 1. So, the last term $f_{kk}(x,y)$ can be calculated as follows (equation 10).

$$f_{kk}(x,y) = 1 - (f_{ii}(x,y) + f_{jj}(x,y)) \tag{10}$$

By finally substituting equation 5 and equation 6 into equation 8 and equation 9, the result is a fibre orientation tensor, depending on the angle and radius f(r,ϕ) in the coordinate system x'-y'. Since the loading direction is defined by the loading angle ϕ, (in our case 45°), a transformation from the x'-y' coordinates to this direction has to be done. Using x or y-value (without transformation) would lead to an overestimation (in this case of 0.19) or underestimation (in this

case of 0.20) of the fibre orientation (figure 17) for a material parameter. So the local resulting tensor (f_{ii}, f_{jj} and f_{kk} for the investigated position) is transformed from the local $x' - y'$-axis system ($T(x, y)$) to the main loading direction ($a_{i,j}$) by using a rotation matrix R (equation 11).

$$a_{i,j} = R \cdot T(x, y) \tag{11}$$

For the strength calculations, the fibre orientation in the main loading direction is considered leading to a main improvement in material parameter determination (figure 17). The results show a deviation of 0.1 (15%) or rather 0.25 (38%) between the measured values and the model without using the proposed calculation method, shown in figure 17. The calculation of the fibre orientations in the main loading direction from the 45° extracted specimens for

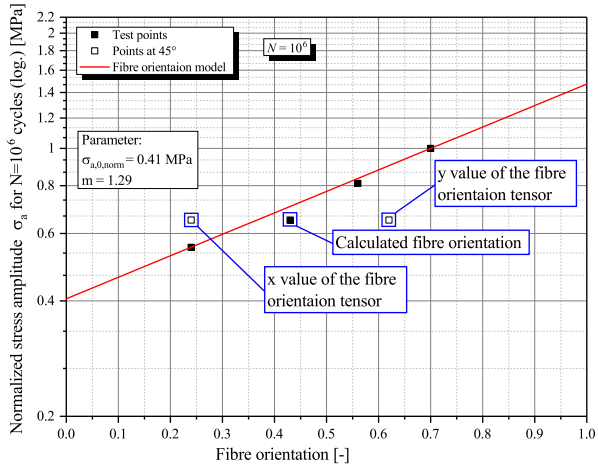

FIGURE 17 Influence of fibre orientation to fatigue strengths

material model calibrations is based on the fibre orientation of failure positions. Consequently, the specimen sizes and shapes are important for material data evaluation. With a reduction of the investigated radius (e.g. specimen size), the fibre orientation tends to those of the plate centre, independent of the loading angle. Finally, the local fibre orientation can be calculated for every loading angle and fracture position, shown in figure 18. The results of the calculations show, that a decreasing radius of the circle, representing the fracture position, shown in figure 16, effects a homogenous fibre orientation, independent of the loading angle. So, specimens extracted from the centre of the plate with a fracture point in the specimen's centre, show a small difference between the fibre orientations and the loading angle. This results in an inaccurate material model calibration, which can be improved by using the proposed method.

5 | CONCLUSION AND OUTLOOK

Tensile and fatigue tests have been performed on specimen, extracted from an injection moulded plate. For the determination of the local material properties, the fibre orientation has been measured with μCT. For the description

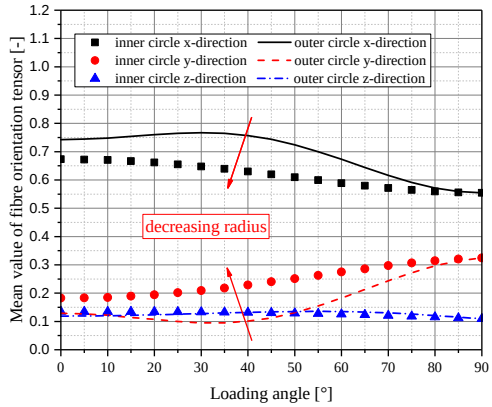

FIGURE 18 Fibre orientation, depending on the loading direction and fracture position

of the fatigue behaviour, the *Tsai-Hill-criterion* and the *Gaier criterion* have been investigated. It can be shown, that there is a main influence in the material properties, depending on the position of the specimens along a plate. So, the local fibre orientation of the failure areas needed to be considered for the fatigue models. The model calibration should be performed by using strength values with a high range in the fibre orientation. As a consequence of this awareness, as long specimens as possible or small specimens with a wide distribution on the plate should be taken. This method only works properly if enough measured fibre orientation points are available. If a plate is characterized, the proposed method can be used for every loading angle and position on the plate. Further, it is reliable to use different specimen shapes and sizes. Our research could be an useful aid for material modelling engineers, because the consideration of the effective material behaviour in the models improves the estimation accuracy for e.g. lifetime estimation. Further studies, which take the fibre orientation over whole plate into account, have to be performed. Additionally different materials and plate shapes should be investigated to confirm these findings. In case of a non constant fibre orientation along the flow path, also this direction need to be considered in the model by replacing the constant $P(x)$ and $O(x)$ with a function to produce a tensor field T(x,y).

Acknowledgements

The research work of this paper was performed at the Chair of Mechanical Engineering at the Montanuniversität of Leoben in collaboration with the Polymer Competence Center Leoben GmbH (PCCL, Austria) within the framework of the COMET-program of the Austrian Ministry of Traffic, Innovation and Technology with contribution by Borealis Polyolefine GmbH, Engineering Center Steyr GmbH & CoKG (MAGNA Powertrain ECS), EVONIK Industries AG, Schaeffler Technologies AG & Co KG, Volkswagen AG as well as EMS-Chemie AG (EMS-GRIVORY) as associated partner. The PCCL is founded by the Austrian Government and the State Governments of Styria, Lower and Upper Austria.

Data availability

The data that support the findings of this study are available from the corresponding author upon reasonable request.

references

[1] Advani Suresh G , Tucker III Charles L . The Use of Tensors to Describe and Predict Fiber Orientation in Short Fiber Composites. Journal of Rheology 1987;31(8):751–784.

[2] Bernasconi A, Cosmi F, Dreossi D. Local anisotropy analysis of injection moulded fibre reinforced polymer composites. Composites Science and Technology 2008;68(12):2574–2581.

[3] Bernasconi A, Conrado E, Cavallaro A, Hine PJ. A Local Stress Analysis of The Effect of Fibre Orientation on The Fatigue Behaviour of a Short Fibre Reinforced Polyamide. In: ICCM, editor. 20th International Conference on Composite Materials; 2015. .

[4] Hartl AM, Jerabek M, Lang RW. Effect of fiber orientation, stress state and notch radius on the impact properties of short glass fiber reinforced polypropylene. Polymer Testing 2015;43:1–9.

[5] Bernasconi A, Cosmi F, Zappa E. Combined effect of notches and fibre orientation on fatigue behaviour of short fibre reinforced polyamide. Strain 2010;46(5):435–445.

[6] Caton-Rose P, Hine PJ, Costa F, Jin X, Wankg J, Parveen B. Measurement and Prediction of Short Glass Fibre Orientation in Injection Moulding Composites. Sankaran2012Venice: ECCM15; 2012. .

[7] Stadler G, Primetzhofer A, Pinter G, Grün F. Investigation of fibre orientation and notch support of short glass fibre reinforced thermoplastics. International Journal of Fatigue 2020;131:105284.

[8] Belmonte E, de Monte M, Hoffmann CJ, Quaresimin M. Damage initiation and evolution in short fiber reinforced polyamide under fatigue loading: Influence of fiber volume fraction. Composites Part B: Engineering 2017;113:331–341.

[9] Guster C, Pinter G, Eichlseder W, Lang RW. Effects of temperature and moisture on the tensile/tensile fatigue behavior of an injection molded sgf-reinforced partial aromatic polyamid. Proceedings of the 12th International Conference on Fracture (ICF 12), Ottawa 2009;.

[10] Kawai M, Takeuchi H, Taketa I, Tsuchiya A. Effects of temperature and stress ratio on fatigue life of injection molded short carbon fiber-reinforced polyamide composite. Composites Part A: Applied Science and Manufacturing 2017;98:9–24.

[11] Mortazavian S, Fatemi A. Fatigue behavior and modeling of short fiber reinforced polymer composites including anisotropy and temperature effects. International Journal of Fatigue 2015;77:12–27.

[12] Nanying Jia, Val A Kagan. Effects of time and temperature on the tension-tension fatigue behavior of short fiber reinforced polyamides. Polymer Composites 1998;(4):408–414.

[13] Malpot A, Touchard F, Bergamo S. An investigation of the influence of moisture on fatigue damage mechanisms in a woven glass-fibre-reinforced PA66 composite using acoustic emission and infrared thermography. Composites Part B: Engineering 2017;130:11–20.

[14] Launay A, Marco Y, Maitournam MH, Raoult I. Modelling the influence of temperature and relative humidity on the time-dependent mechanical behaviour of a short glass fibre reinforced polyamide. Mechanics of Materials 2013;56:1–10.

[15] De Monte M, Moosbrugger E, Jaschek K, Quaresimin M. Multiaxial fatigue of a short glass fibre reinforced polyamide 6.6 - Fatigue and fracture behaviour. International Journal of Fatigue 2010;32(1):17–28.

[16] Klimkeit B, Nadot Y, Castagnet S, Nadot-Martin C, Dumas C, Bergamo S, et al. Multiaxial fatigue life assessment for reinforced polymers. International Journal of Fatigue 2011;33(6):766–780.

[17] Launay A, Maitournam MH, Marco Y, Raoult I. Multiaxial fatigue models for short glass fibre reinforced polyamide. Part II: Fatigue life estimation. International Journal of Fatigue 2013;47(0):390–406.

[18] Primetzhofer A, Stadler G, Pinter G, Grün F. Lifetime assessment of anisotropic materials by the example short fibre reinforced plastic. International Journal of Fatigue 2018;.

[19] Azzi VD, Tsai SW. Anisotropic strength of composites. Experimental Mechanics 1965;5(9):283–288. https://doi.org/10.1007/BF02326292.

[20] Gaier C, Dannbauer H, Werkhausen A, Wahlmüller R. Fatigue life prediction of short fiber reinforced plastic components. In: Curran Associates, editor. 8th annual Automotive Composites Conference and Exhibition (ACCE 2008) SPE Automotive & Composites Division; 2009. .

[21] Gaier C, Fleischer H, Guster C, Pinter G. Einfluss von Faserorientierung Temperatur und Feuchtigkeit auf das Ermüdungsverhalten von kurzfaserverstärkten Thermoplasten. MP Material Testing 2010;52(7-8):534–542.

[22] Mösenbacher A, Brunbauer J, Pichler PF, Guster C, Pinter G. Modelling and validation of fatigue life calculation method for short fibre reinforced injection moulded parts. In: ECCM, editor. 16th European Conference of Composite Materials; 2014. .

[23] Bernasconi A, Conrado E, Hine P. An experimental investigation of the combined influence of notch size and fibre orientation on the fatigue strength of a short glass fibre reinforced polyamide 6. Polymer Testing 2015;47:12–21.

[24] Dean A, Grbic N, Rolfes R, Behrens B. Macro-mechanical modeling and experimental validation of anisotropic, pressure- and temperature-dependent behavior of short fiber composites. Composite Structures 2019;211:630–643.

[25] Hine PJ, Davidson NC, Duckett RA, Ward IM. Measuring the fibre orientation and modelling the elastic properties of injection-moulded long-glass-fibre-reinforced nylon. Composites Science and Technology 1995;53(2):125–131.

[26] Bernasconi A, Cosmi F, Hine PJ. Analysis of fibre orientation distribution in short fibre reinforced polymers: A comparison between optical and tomographic methods. Composites Science and Technology 2012;72(16):2002–2008.

[27] Brunbauer J, Mösenbacher A, Guster C, Pinter G. Fundamental influences on quasistatic and cyclic material behavior of short glass fiber reinforced polyamide illustrated on microscopic scale. Journal of Applied Polymer Science 2014;131(19):n/a–n/a.

[28] Salaberger D. Micro-structure of discontinuous fibre polymer matrix composites determined by X-ray computed tomography. PhD thesis, Wien; 2019.

[29] Radaj D, Vormwald M. Ermüdungsfestigkeit: Grundlagen für Ingenieure. 3 ed. Berlin [u.a.]: Springer; 2007.

[30] Bernasconi A, Davoli P, Basile A, Filippi A. Effect of fibre orientation on the fatigue behaviour of a short glass fibre reinforced polyamide-6. International Journal of Fatigue 2007;29(2):199–208.

[31] de Monte M, Moosbrugger E, Quaresimin M. Influence of temperature and thickness on the off-axis behaviour of short glass fibre reinforced polyamide 6.6 – cyclic loading. Composites Part A: Applied Science and Manufacturing 2010;41(10):1368–1379.